



USING AIR-COUPLED SENSORS TO MEASURE DEPTH OF A SURFACE-BREAKING CRACK IN CONCRETE

Seong-Hoon Kee and Jinying Zhu

Citation: [AIP Conference Proceedings](#) **1096**, 1497 (2009); doi: 10.1063/1.3114134

View online: <http://dx.doi.org/10.1063/1.3114134>

View Table of Contents:

<http://scitation.aip.org/content/aip/proceeding/aipcp/1096?ver=pdfcov>

Published by the [AIP Publishing](#)

Articles you may be interested in

[Crack depth measurement in concrete using diffuse ultrasound](#)

AIP Conf. Proc. **1430**, 1485 (2012); 10.1063/1.4716391

[AIR-COUPLED SURFACE WAVE TRANSMISSION MEASUREMENT ACROSS A PARTIALLY CLOSED SURFACE-BREAKING CRACK IN CONCRETE](#)

AIP Conf. Proc. **1335**, 169 (2011); 10.1063/1.3591853

[Using air-coupled sensors to determine the depth of a surface-breaking crack in concrete](#)

J. Acoust. Soc. Am. **127**, 1279 (2010); 10.1121/1.3298431

[Crack Depth Measurement in Concrete Using Surface Wave Transmission](#)

AIP Conf. Proc. **657**, 1125 (2003); 10.1063/1.1570259

[Measurement of surface wave transmission coefficient across surface-breaking cracks and notches in concrete](#)

J. Acoust. Soc. Am. **113**, 717 (2003); 10.1121/1.1537709

USING AIR-COUPLED SENSORS TO MEASURE DEPTH OF A SURFACE-BREAKING CRACK IN CONCRETE

Seong-Hoon Kee and Jinying Zhu

Department of Civil, Architectural, and Environmental Engineering, the University of Texas, Austin, TX 78712-0273

ABSTRACT. Previous studies show that surface wave transmission ratio across a surface breaking crack in concrete can be used as an indicator of the crack depth. However, due to inconsistent sensor coupling condition on rough concrete surface, reliable measurement of the transmission ratio is still a challenging task. In this study, the air-coupled sensing method is proposed as a solution to this problem. Without direct contact between sensors and the testing surface, the air-coupled sensing not only allows rapid testing speed, but also enables more consistent signal measurement owing to removal of sensor coupling variation. The latter feature is especially valuable to wave transmission measurement. This paper first presents results from a numerical analysis (FEM model). Based on the results, a simplified algorithm is proposed for surface wave transmission ratio calculation. A calibration curve between the transmission ratio and normalized crack depth (actual crack depth/wavelength) is obtained. Experimental study using the air-coupled sensing method verifies the validity of the curve.

Keywords: Air-Coupled Sensor, Leaky Rayleigh Wave, Surface-Breaking Crack, Concrete
PACS: 43.20.El, 43.20.Hq, 43.35.Pt.

INTRODUCTION

The early stage of damage in reinforced concrete (RC) structures generally begins with several types of surface-breaking cracking. Appearance of cracks on the RC members designed in accordance with current building codes does not necessarily imply the structural failure; however, it causes many serviceability and durability problems, e.g., stiffness degradation, corrosion of the steel reinforcement, infiltration of moisture. These effects make cracks deeper and wider, and lead to early malfunction of concrete structures. Evaluating the extent of cracks in RC members is of importance to estimate the degree of deterioration, and to determine the appropriate rehabilitation scheme.

Previous studies showed that surface wave transmission coefficient T_r across a surface breaking crack in a solid can be used as an indicator of the crack depth in non-destructive evaluation. Using ultrasonic transducers, Viktorov [1] experimentally developed the relationship between the surface wave transmission coefficient and the normalized crack depth h/λ , i.e., the ratio of crack depth to the wavelength, for a surface-breaking crack in a solid. Angel and Achenbach [2] obtained T_r and h/λ relation based on an analytic model

considering diffraction and scattering of Rayleigh wave by a surface-breaking crack in a homogeneous elastic half-space domain. For concrete, a heterogeneous but globally isotropic material, Hevin et al. [3] obtained the transmission ratio of surface wave in frequency domain using numerical simulations, and proposed the cut-off frequency ($h/\lambda = 0.3$) method to estimate crack depth. Popovics and Song et al. [4-5] also obtained the Tr and h/λ relationship through experiments and boundary element analysis. For surface wave transmission measurements, they used a self-compensating procedure [6] to eliminate surface coupling inconsistency and geometric attenuation effects. They found that the relationship is not affected by crack width and the shape of crack tip.

The self-compensating technique improves the consistency of surface wave measurement by measuring the transmission ratio from two opposite directions (the detail is explained in experimental section and references 4-5). However, the low resonance frequencies induced by installation of contact sensors (accelerometers) prevent accurate measurement of surface wave amplitude, especially in the low frequency range.

Air-coupled sensors have been successfully used to measure leaky Rayleigh waves or Lamb waves in concrete by Zhu and Popovics [7]. Compared to contact sensors, air-coupled sensors have the following advantages: 1) the non-contact sensing technique eliminates the sensor coupling problem, and thus gives more consistent measurement results; and 2) the non-contact feature makes it possible to perform rapid scanning of large civil engineering structures. Therefore, application of air-coupled sensors in conjunction with self-compensating technique will improve the signal quality and test efficiency in surface wave transmission measurements for concrete.

In this study, we used numerical simulations to investigate critical parameters that affect the surface wave transmission measurement. The parameters include the depth of crack h , impact duration time of the source, and locations of sensors. The crack depth used in numerical simulations varies from 10 to 150 mm, and the impact duration time of the point source varies from 20 to 200 μ s. This type of setup gives a range of h/λ about 0-4, which covers the typical frequency range of surface wave transmission measurement. To minimize near-field effects caused by crack tip scattering on surface wave measurement, we also suggested the optimal sensor location as a function of h/λ . The obtained Tr and h/λ relationship is compared with the analytic solution given by Angel and Achenbach [2]. Then a simplified algorithm is proposed for surface wave transmission ratio calculation. In the experimental study, data were collected from an artificial crack with varying depth (10-100 mm) in a concrete slab. The experimental results validated the numerical analysis.

NUMERICAL SIMULATION

Finite Element Model

Finite element method (FEM) was used to investigate surface wave attenuation caused by a surface-breaking crack in a solid. The solid was modeled by 4-node axi-symmetry elements (CAX4) in the commercial program ABAQUS 6.7-1, with mesh size of 5mm. The finite element model is shown in Fig. 1. Sixteen models were analyzed for crack depth h ranging from 0 to 150mm in a 10mm step. To reduce wave reflections from boundaries, absorption boundary (CINAX4) elements were applied.

For the investigated wavelength (>40 mm) in this study, concrete can be regarded as a homogeneous material. The material properties are: Young's modulus of 33630 MPa, Poisson's ratio of 0.222, and mass density of 2400 kg/m³. The corresponding velocities of P-, S-, and Rayleigh waves are 4050, 2420, and 2215 m/s, respectively.

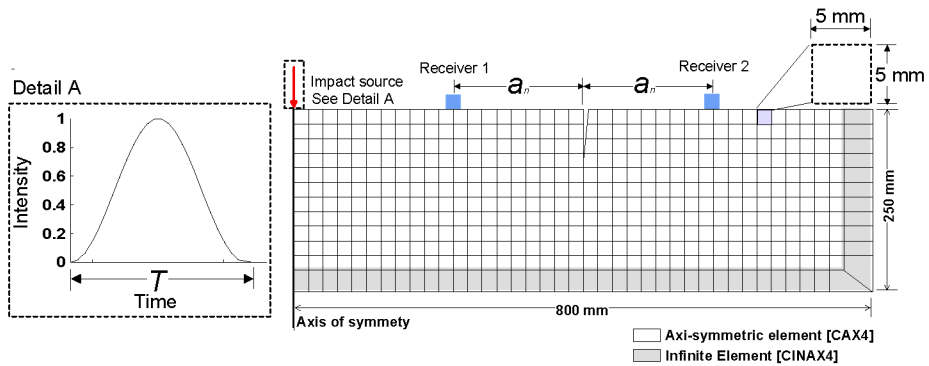


FIGURE 1. Axi-symmetric finite element model for elastodynamic transient analysis.

The force function of the transient impact point source is $f(t) = \sin^2(\pi/T)$, where T is the duration time ranging from 20 to 200 μs in a step of 20 μs . The impact source is 400 mm from the crack opening on the concrete surface. To study the near field effect caused by the crack tip scattering, various sensor locations on surface of concrete were considered.

Near Field Effect

Figure 2 shows vertical displacement responses measured before and after the crack opening on the solid surface. The distances from the crack opening are -20, -15, -10, -5, 0, 5, 10, 15, 20, 25, and 30 mm, where negative values indicate locations before the crack. Figure 2(a) shows results on a crack free model, while 2(b) for a model with a 40 mm deep crack. The impact duration of the point source is 20 μs . In Fig. 2(b), amplification of vertical displacements can be observed in the vicinity of the crack opening, which is regarded as the near field effect caused by crack tip scattering.

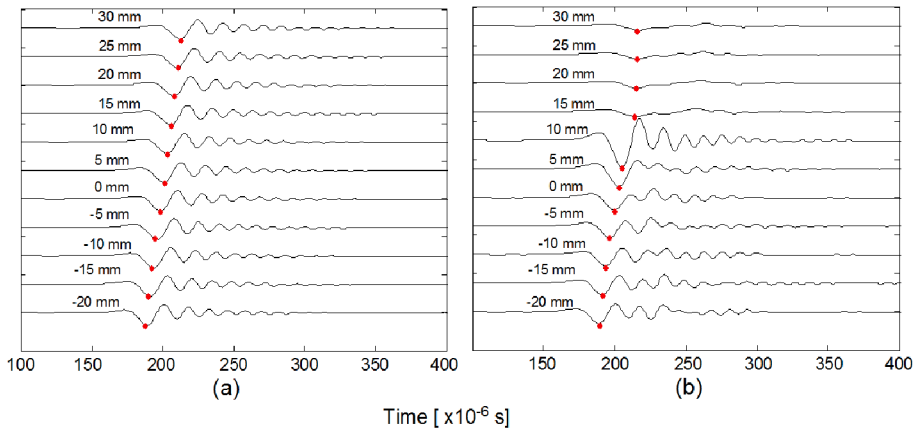


FIGURE 2. Vertical displacement measured at various distances from the crack opening, where negative values indicate locations before the crack. Results are from (a) a crack free medium, and (b) a model with a 40 mm deep crack. The impact duration of the point source is 20 μs .

To investigate the near field effect of the surface-breaking crack with varying duration of impact point sources (20 ~ 200 μ s) and depth of crack (0 ~ 150 mm), an amplification coefficient (APC) is defined. In this study, APC is defined as the peak amplitude ratio between the vertical displacement obtained on the cracked model (U_{zi}) and that on the crack free model (U_{z0}), as shown in Eq. (1). U_{zi} and U_{z0} are marked with dots in Fig. 2.

$$APC(x/\lambda) = \frac{U_{zi}(x/\lambda)}{U_{z0}(x/\lambda)} \quad (1)$$

Figure 3 shows the amplification coefficient curves versus the normalized distance x/λ from the crack opening for various crack depths. Analysis shows that the APC curves depend on the distance from the crack x , the crack depth h and wavelength λ . The curves in Fig. 3 indicate that the amplification coefficient oscillates in the near crack region (near field), while it converges to a constant value in the far field for large x/λ . The near field size depends on the relative crack depth h/λ . Previous research [3-5] found that the surface wave transmission curve decreases monotonically with increasing frequency in the range of $h/\lambda=0\sim 1/3$. Within this range surface wave transmission is sensitive to the change of crack depth. Based on the results shown in Fig. 3, in the range of $h/\lambda=0\sim 1/3$, the near field size can be expressed as

$$(a_n/\lambda) = 1.8 h/\lambda + 0.1 \text{ for } h/\lambda \leq 1/3 \quad (2)$$

where a_n is the near field size measured from the crack opening. To reduce the effects of crack tip scattering, surface wave transmission should be measured in far field regions, i.e., the sensor to crack opening spacing should be larger than a_n . For $h/\lambda=1/3$, the near field size calculated from Eq. (2) is $a_n = 0.7 \lambda$.

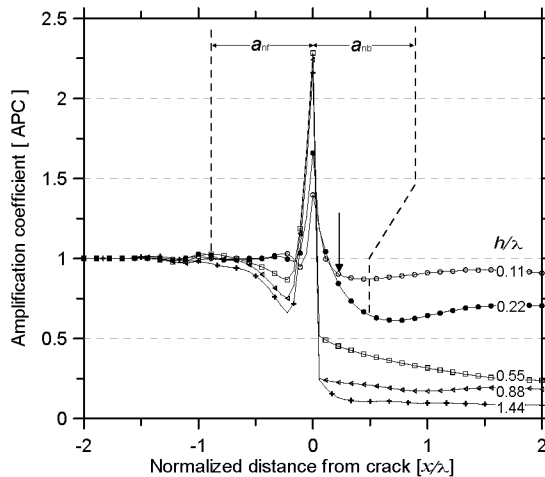


FIGURE 3. Amplification coefficient (APC) and normalized distance (x/λ) relation with varying normalized crack depth h/λ .

Calculation of Transmission Coefficient

The surface wave transmission coefficient is defined as

$$Tr(f, h) = V_2(f, h) / V_1(f, h), \quad (3)$$

where Tr is a transmission coefficient in function of frequency and crack depth, and V_2, V_1 are the frequency domain responses measured at locations Receiver 1 and 2 (see Fig. 1).

Figure 4 shows the normalized surface wave transmission coefficients versus h/λ . These data are obtained from the FEM models with various crack depths and impact duration time. To eliminate geometric attenuation effects, the transmission coefficient $Tr(f, h)$ is normalized by the transmission obtained from the crack free model $Tr(f, 0)$. For comparison purpose, the analytical result given by Angel and Achenbach [2] is also shown in Fig. 4. It can be seen that the numerical and analytical results show good agreement. The transmission coefficient monotonically decreases with increasing crack depth in the range of $h/\lambda = 0 \sim 1/3$. When h/λ is between $1/3$ and 1.0 , Tr shows oscillation with h/λ . Tr is very low when $h/\lambda > 1.0$, which indicates that surface waves cannot transmit through the crack if the wavelength is shorter than the crack depth.

To find the averaged trend of Tr_n vs. h/λ relation, a non-linear regression curve based on Gaussian function is shown in Fig. 4. The regression equation is

$$Tr_n = -0.1524 e^{-\left(\frac{h/\lambda - 0.3319}{0.0799}\right)^2} - 1.404 \times 10^{11} e^{-\left(\frac{h/\lambda - 37.67}{7.306}\right)^2} + 0.6055 e^{-\left(\frac{h/\lambda - 0.004826}{0.3172}\right)^2} \quad (4)$$

which agrees well with the analytical curve in the range of $h/\lambda = 0 \sim 0.4$.

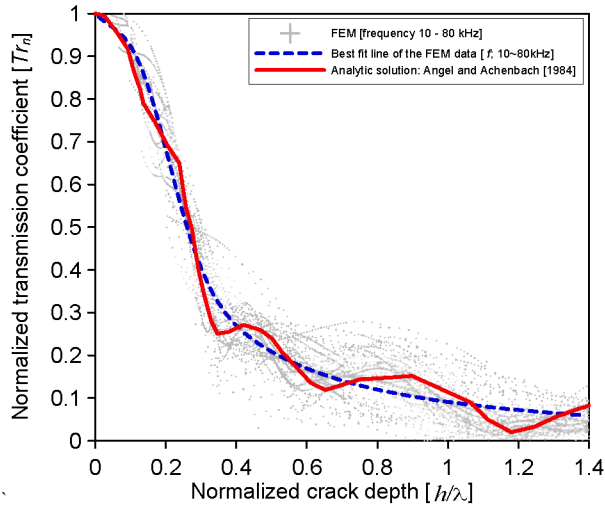


FIGURE 4. Normalized transmission coefficient and normalized crack depth based on FE and analytic solution.

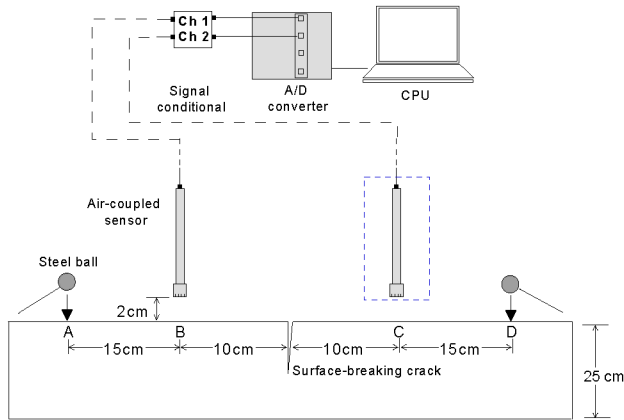


FIGURE 5. Test setup and data acquisition system.

EXPERIMENTAL VERIFICATION

Test Setup and Data Acquisition System

The schematic view of the test setup is shown in Fig. 5. Two air-coupled sensors were used to measure the leaky surface waves propagating along the concrete surface. The air-coupled sensor has the following properties: nominal diameter of 6 mm; ± 2 db flat frequency response over 4 Hz to 80 kHz; resonance frequency around 83 kHz. The sensors are 20 mm from the concrete surface.

A 250 mm thick concrete specimen was cast in the laboratory at the University of Texas Austin. Notch-typed cracks with depths varying from 10 to 100 mm were generated in the specimen by placing 0.5 mm thick iron sheet before casing concrete. The iron sheet was removed from the concrete 12 hours later. Previous research [4-5] has shown that crack types or crack width do not affect the surface wave transmission measurement.

The self-compensating technique [6] was used to measure surface wave transmission across a crack in concrete. The test setup is shown in Fig. 5. First, the surface waves generated by an impact load at location *A* were recorded by sensors at locations *B* and *C*. The signals are denoted as V_{AB} and V_{AC} . Therefore the wave transmission between locations *B* and *C* can be calculated from these two signals and denoted as T_{BC} . To eliminate the unsymmetrical effect caused by sensor coupling, an impact load was then applied at location *D*, and the signals recorded by the sensors at locations *B* and *C* are denoted as V_{DB} and V_{DC} . The transmission ratio between locations *C* and *B* are defined as T_{CB} . The surface wave transmission function is defined as

$$|Tr(f)| = \sqrt{\frac{V_{AC}V_{DB}}{V_{AB}V_{DC}}} \quad (5)$$

All analyses were performed in frequency domain. A *Hanning* window was applied to the time domain signal to extract the surface wave component.

Three different sizes of steel balls were used as impact sources. They generate incident surface waves with center frequencies around 18, 20 and 25 kHz. The acquired signals were digitized at sampling frequency of 10 MHz using NI-PXI 5105 oscilloscope. To

acquire consistent and reliable signal data, five signal data sets were collected to obtain averaged transmission coefficients. The signal consistency of the data sets is defined as

$$SC(f) = \frac{\sqrt[N]{\prod_{i=1}^N T_{BCi}(f)}}{\sum_{i=1}^N T_{BCi}(f) / N} \quad (6)$$

where N is the number of data sets ($N=5$ in this study).

Transmission Coefficient and Normalized Crack Depth Relation

Figure 6(a) shows the normalized transmission coefficient Tr_n versus h/λ curves obtained from experiments on the concrete specimen. Data were collected in the far-field for various crack depths. The center frequency of the impact source is around 20 kHz. The experimental results show good agreement with the FEM simulation and the analytic solution. The agreement is especially good for shallow cracks, $h=20$ mm and 30 mm, when the impact source contains enough low frequency energy to cover the range of $h/\lambda < 1/3$. For deep cracks, the source should contain more low frequency contents to give reliable transmission measurement in $h/\lambda < 1/3$ range.

Signals contain the highest energy at their center frequencies. Therefore, measurements around the center frequencies provide most reliable results. Based on this assumption, we proposed a simplified algorithm to measure and calculate the surface wave transmission. Instead of calculating wave transmission for all frequencies, we calculate Tr at the center frequency only. With the measured surface wave transmission ratio at the center frequency, h/λ can be directly found from the established Tr - h/λ curve. If the surface wave velocity is known, then λ can be calculated, and the crack depth h is determined. Figure 6(b) shows the experimental data based on center frequency transmission measurement for four crack depths, using three different impact sources. The experimental data based on center frequency measurement are in good agreement with the theoretical Tr - h/λ curve. Therefore, the surface wave transmission measurement with simplified algorithm is a potential in-situ NDT method to estimate the crack depth in concrete.

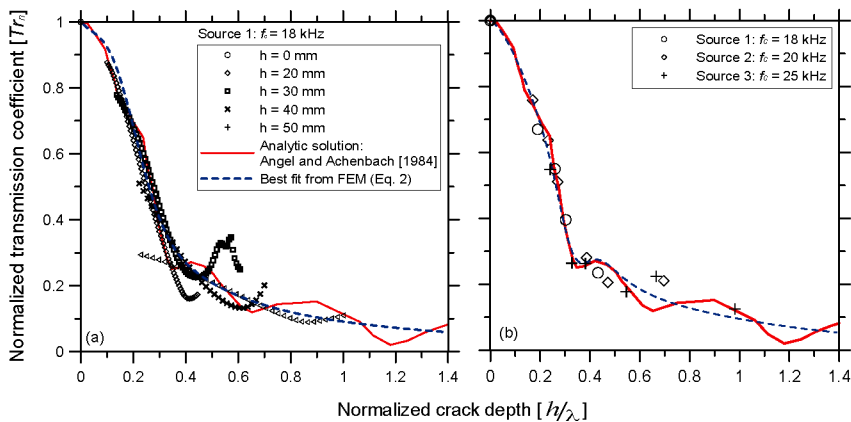


FIGURE 6. Experimental curves of normalized transmission coefficient vs. normalized crack depth: (a) transmission curves obtained on crack depths of 20 to 50mm; (b) transmission measurement based on the center frequency of incident waves.

SUMMARY

1) The transmission function based on finite element analysis agrees well with the analytic solution given by Angle and Achenbach [2]. The finite element model in this study can be extended to more complex problems where analytic solution does not exist.

2) Surface wave transmission method can be used to estimate crack depth when h/λ is less than 1/3. For larger h/λ , the surface wave transmission coefficient becomes insensitive to the change of h/λ .

3) Near field size depends on crack depth and surface wavelength. To obtain reliable and consistent transmission coefficient, measurement should be taken in far field regions.

4) The air-coupled sensors show good signal consistency.

5) A simplified algorithm based on center frequency is suggested in this paper. Experimental study showed effectiveness of the method to estimate crack depth in concrete.

REFERENCES

1. I.A. Viktorov, "Rayleigh Waves and Lamb waves-Physical Theory and Application," Plenum, New York (1967), pp. 57-65.
2. Y.C. Angel, and J.D. Achenbach, *J. Acoust. Soc. Am.*, **75** (2), pp. 313-319 (1984).
3. G. Hevin, O. Abraham, H.A. Petersen, M. Campillo, *NDT & E Int.*, **31** (4), pp. 289-298 (1998).
4. J. S. Popovics, W-J. Song, M. Ghandehari, K. V. Subramaniam, J. D. Achenbach, and S. P. Shah, *ACI Material journal*, **97**, **2**, pp. 127-135 (2000).
5. W-J. Song, J. S. Popovics, J. C. Aldrin, and S. P. Shah, *J. Acoust. Soc. Am.*, **113** (2), pp. 717-725 (2003).
6. J. D. Achenbach, I. N. Komsky, Y. C. Lee, and Y. C. Angel, *J. Nondestr. Eval.*, **11** (2), pp. 103-108 (1992).
7. J. Zhu, and J. S. Popovics, *J. Acoust. Soc. Am.*, **116** (4), pp. 2101-2110 (2004).